Proceedings 10th NUMGE 2023
10th European Conference on Numerical Methods in Geotechnical Engineering
Zdravkovic L, Kontoe S, Taborda DMG, Tsiampousi A (eds)

https://doi.org/10.53243/NUMGE2023-362

Numerical assessment of enhanced urban-train support systems

J.M. Mayoral[1], N. Olivera[1], S. Tepalcapa[1], A. Román[2], M. Alcaraz[1]

[1]*Institute of Engineering, National University of Mexico, Mexico City, Mexico*
[2]*Instituto Tecnológico y de Estudios Superiores de Monterrey, Mexico City, Mexico*

ABSTRACT: Current modern performance based-design of train-track supports in urban areas is based on estimating and controlling induced stresses to which it may be subjected. However, these stresses are often obtained through methods based on semi-empirical equations for which areas of opportunity have been identified. Likewise, these methodologies do not consider the calculation of deformations (i.e., elastic and plastic), so they cannot evaluate the system's actual performance. This paper presents the results obtained from numerical simulations with three-dimensional finite-difference models developed to assess the behavior of typical materials that constitute the support of urban train systems for an original support system and an enhanced one. Several load scenarios were considered, and the substitution of some of its elements (i.e., base material and ballast) was evaluated to improve the system's performance. The results from the numerical study were compared with some of the most used equations in practice. The developed models made it possible to calculate the actual stress distribution and the accumulation of plastic deformations due to cyclic loading acting on the track with and without enhancement. With the results obtained, it is shown the importance of evaluating the permanent deformation (i.e., plastic) to avoid costly maintenance and potentially unsafe designs.

Keywords: Ballasted railway tracks; Numerical modelling; Finite difference method; Stress analysis.

1 INTRODUCTION

Ballast, and other granular rail track support (base-type) materials are subjected to various factors that affect their performance during the economic life of an urban train. These are mainly because of cyclic loading, including changes in train speed and braking. Several authors have studied the loads generated by the passage of trains which produce higher forces on the track support and lead to excessive deformations. In high-speed trains, the analysis of critical speed is important as it creates a problem like resonance (Sayeed and Shahin, 2022). Also, laboratory tests have been performed (Indraratna and Nimbalkar, 2013; Ramos et al., 2021) to understand the stress-strain behavior of the materials that comprise the support of a track.

The ballast has a key role in the track support and transmits stresses at an allowable bearing capacity level to the underlying base-type material preventing excessive settlement and lateral displacements (Selig and Waters, 1994). Previous studies indicate that the breakage of granular materials such as ballast generated by cyclic loading significantly influences its strength and deformability parameters (Liu and Zou, 2013). Degradation of ballast has effects on track alignment, which increases the possibility of accidents (Das and Bajpai, 2018).

In general, the stresses to which the ballast and the base-type material are subjected are estimated by methods based on semi-empirical equations. Two of the most frequently used methods are presented by AREMA (2010) and Hay (1982). Although the methodology presented by AREMA (2010) has been updated to consider the separation between sleepers (i.e., distribution factor), the velocity and diameter of wheel (i.e., impact factor), these updates were implemented around fifty years ago, and when computing the mean pressure under the sleeper, both methods use the equation developed by Talbot (1920) for the estimation of the pressure distribution with depth to the center of the sleeper. Likewise, both methodologies do not consider the calculation of deformations (elastic and plastic), so they are not able to evaluate the realistic performance of the system in the long term.

This paper presents the results of numerical simulations carried out with three-dimensional finite difference models, where the behavior of typical materials that constitute the track support of urban underground train systems, particularly those located in tunnels, is considered explicitly in the simulation.

The analysis takes into account various loading scenarios to which such systems may be subjected and other factors such as operating speed. The substitution of some of the elements to improve the performance of the system is also evaluated. The results obtained from the numerical models are compared to those obtained with the empirical equations more commonly used in engineering practice to know the level of variability involved in using them.

Based on the analysis of the results of the numerical models, it is clearly observed that permanent deformation (i.e., plastic) occurs due to the cyclic loading acting on the track, which must be assessed to avoid high maintenance costs and potentially unsafe designs.

2 METHODOLOGY

A typical configuration of the track-sleeper system of underground (i.e., in tunnel) urban trains in Mexico was selected and is presented in Figure 1. Three-dimensional finite difference numerical models were developed with the software FLAC^{3D}, which is shown in Figure 2. The mechanical properties of the materials, including strength and deformability, considered in the numerical simulations, were obtained from the technical literature, and are presented in Table 1 (i.e., Burt G.L. 2007; Montiel-Valera et al., 2017; Sayeed and Shahin 2016).

To characterize the cyclic load transmitted by the bogie, it was considered: 1) the maximum sustained load of 147.15 kN per axle (73.57 kN per wheel), 2) a design speed of 85 km/h, 3) a wheel diameter of 0.914m, and 4) an impact factor, IF (Equation 1), of 0.48 as recommended by AREMA (2010). Thus, the cyclic load was applied 1000 times with a frequency of 10 Hz, considering a distance between each axle of 2.40 m.

$$IF = \frac{33V}{100D} \tag{1}$$

where: V = speed in mph; D = wheel diameter in inches.

With respect to the loading scenarios, Figure 3 presents the cases considered (i.e., Case I, II and III). These were proposed based on the operation of the trains, where a higher load concentration was noted on the outer rail track when the train enters a curve, which was assumed for Case III, representing the most unfavorable loading condition. In addition, the replacement of the base-type material with fluid concrete, and the ballast with a ballast of better quality (according to Standard Australian AS2758.7) was evaluated, considering the properties presented in Table 2 (i.e., Cases IV and V). Table 3 presents a summary of the cases analyzed.

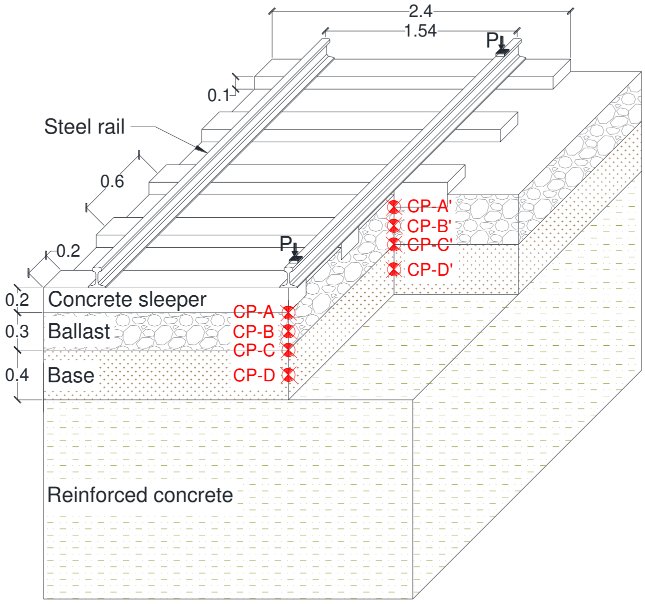

Figure 1. Support system and control point configuration (units in meters)

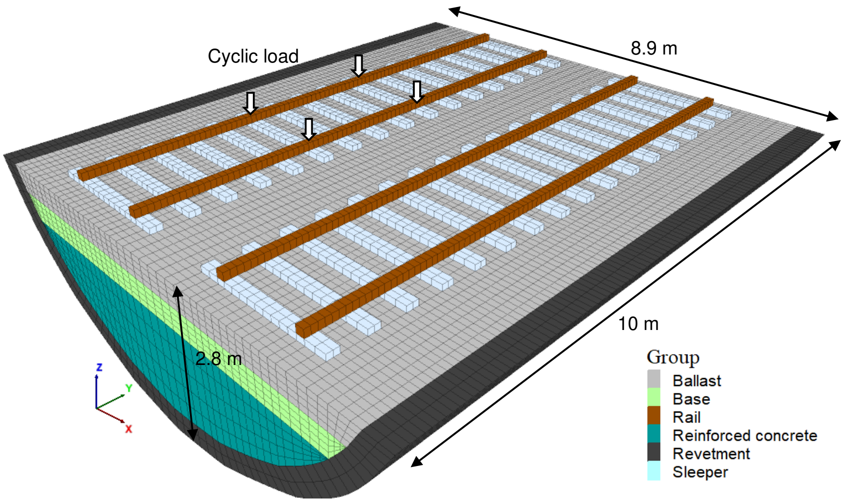

Figure 2. Three-dimensional finite difference model

Table 1. Material properties without enhancement

Group	Constitutive model	γ (kN/m^3)	c (MPa)	ϕ (°)	E (MPa)	υ (-)
Ballast	Cysoil	18.6	0	50	200	0.30
Base	Mohr-Coulomb	17.6	0	43	143	0.35
Concrete	Elastic	22.0			9,590	0.30
Sleeper	Elastic	24.0			47,500	0.18
Rail	Elastic	79.0			210,000	0.30

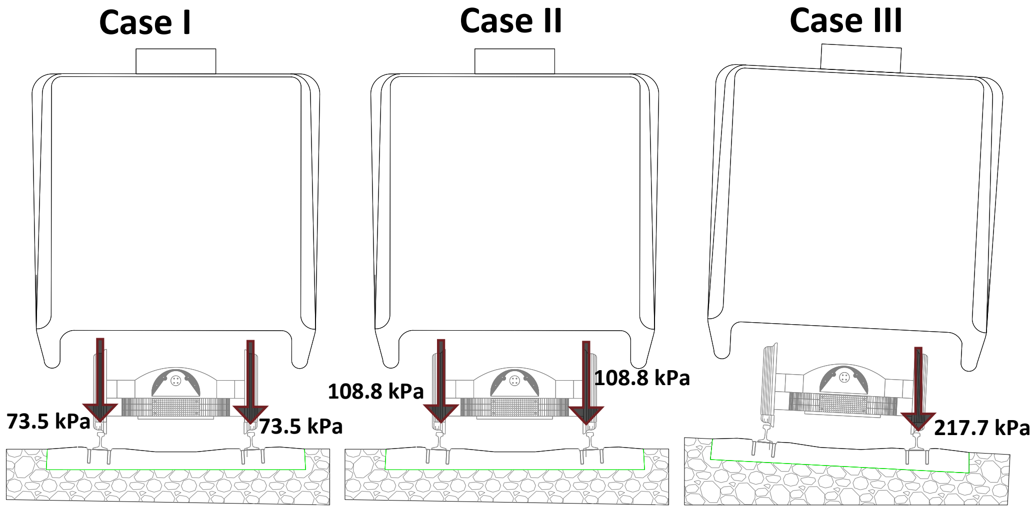

Figure 3. Loads considered

Table 2. Material properties with enhancement

Material	Constitutive model	γ (kN/m^3)	c (MPa)	ϕ (°)	E (MPa)	υ (-)	f'c (MPa)	Reference
Ballast	Cysoil	15.3	0	60	280	0.30	-	Indraratna and Nimbalkar, 2013
Fluid concrete	Mohr-Coulomb	17.1	0.981	0	4561	0.30	1.96	CEMEX, 2022

Table 3. Cases analyzed

Case	Load per wheel (kN)	Impact Factor, IF	Load per wheel with IF (kN)	Substituted material
I	73.57	-	73.57	
II	73.57	0.48	108.89	
III	147.15	0.48	217.78	
IV	147.15	0.48	217.78	Ballast
V	147.15	0.48	217.78	Base-type material and ballast

To consider the accumulation of plastic deformations in each loading cycle, due to the breakage of the ballast particles and the subsequent rearrangement of the ballast particles, the Cysoil constitutive model (Itasca Group Consulting, 2012) was used in the simulation. This is a stress-hardening constitutive model characterized by a frictional Mohr-Coulomb shear envelope (zero cohesion) and an elliptic volumetric cap. The elastic behavior is expressed using Hooke's law. The incremental expression of the law is presented in terms of principal stresses and strains. The yield surface of the model is not fixed in the space of principal stresses, which allows it to expand due to plastic deformations.

The behavior of the model can be adjusted for different behavioral characteristics of soils by selecting the hardening laws. A cap-hardening law allows to capture the volumetric power law behavior observed in isotropic compaction tests; a friction-hardening law, to reproduce the hyperbolic stress-strain law behavior observed in drained triaxial tests; and a compaction/dilation law to model irrecoverable volumetric strain taking place as a result of soil shearing. With respect to damping, viscous boundaries according to the formulation of Lysmer and Kuhlmeyer (1969), were implemented to avoid wave reflection.

3 RESULTS

For each case analized, the vertical stresses, safety factors, FS, and vertical displacements were obtained, considering the deviatoric stresses in the geomaterials and the resistance to shear stress through Equations 2-5, for the base-type material.

$$FS = \frac{\tau_{res}}{\tau_{oct}} \tag{2}$$

$$\tau_{res} = c + p'\tan\varphi \tag{3}$$

$$\tau_{oct} = \frac{\sqrt{(\sigma_1-\sigma_2)^2+(\sigma_2-\sigma_3)^2+(\sigma_1-\sigma_3)^2}}{3} \tag{4}$$

$$p' = \frac{\sigma_1+\sigma_2+\sigma_3}{3} \tag{5}$$

where: τ_{res}= strength stress; τ_{oct} = octahedral shear stress, σ_1, σ_2 y σ_3 = principal stress; c = cohesion; p' = average effective stress; φ = friction angle.

Figure 4 presents the contours of vertical stress for case I. As can be seen, the simulated loads do not influence the forces on the right-hand side, so it is justified to simulate the transit of the trains on one side only, in order to study the problem. Figure 5 presents the contours of vertical stresses for cases II, III, IV and V. Table

4 present the maximum stress in each control point. As can be seen the maximum stresses do not appear below the sleepers where the load was applied. Therefore, it is necessary to study the behavior of these materials through three-dimensional models. Regarding to case IV, the stress magnitudes obtained increase, when the ballast is replaced by one with better properties. This is due to the significant change in the redistribution of stresses transmitted to the base material. In case V, the maximum stress obtained under the sleeper is the lowest with respect to the cases under the same load conditions (i.e., III and IV), however, the system experiences less deformation, in almost all directions, except for the transverse direction (x axis).

Table 5 presents the minimum safety factors for the base material and the fluid concrete. As can be seen, the highest FS value is presented for case V (i.e. ≥3), which is due to the new material type base have better strength. The other cases presented lower values of FS, as they have materials with lower strength, being the case III the most unfavorable. Although with the FS it is possible to know part of the behavior that the track will have, this does not ensure satisfactory performance, for which it is necessary to calculate the corresponding plastic deformations.

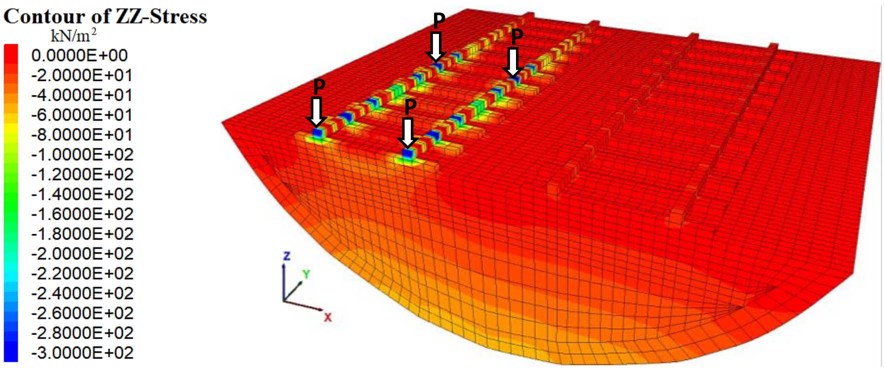

Figure 4. Vertical stress case I

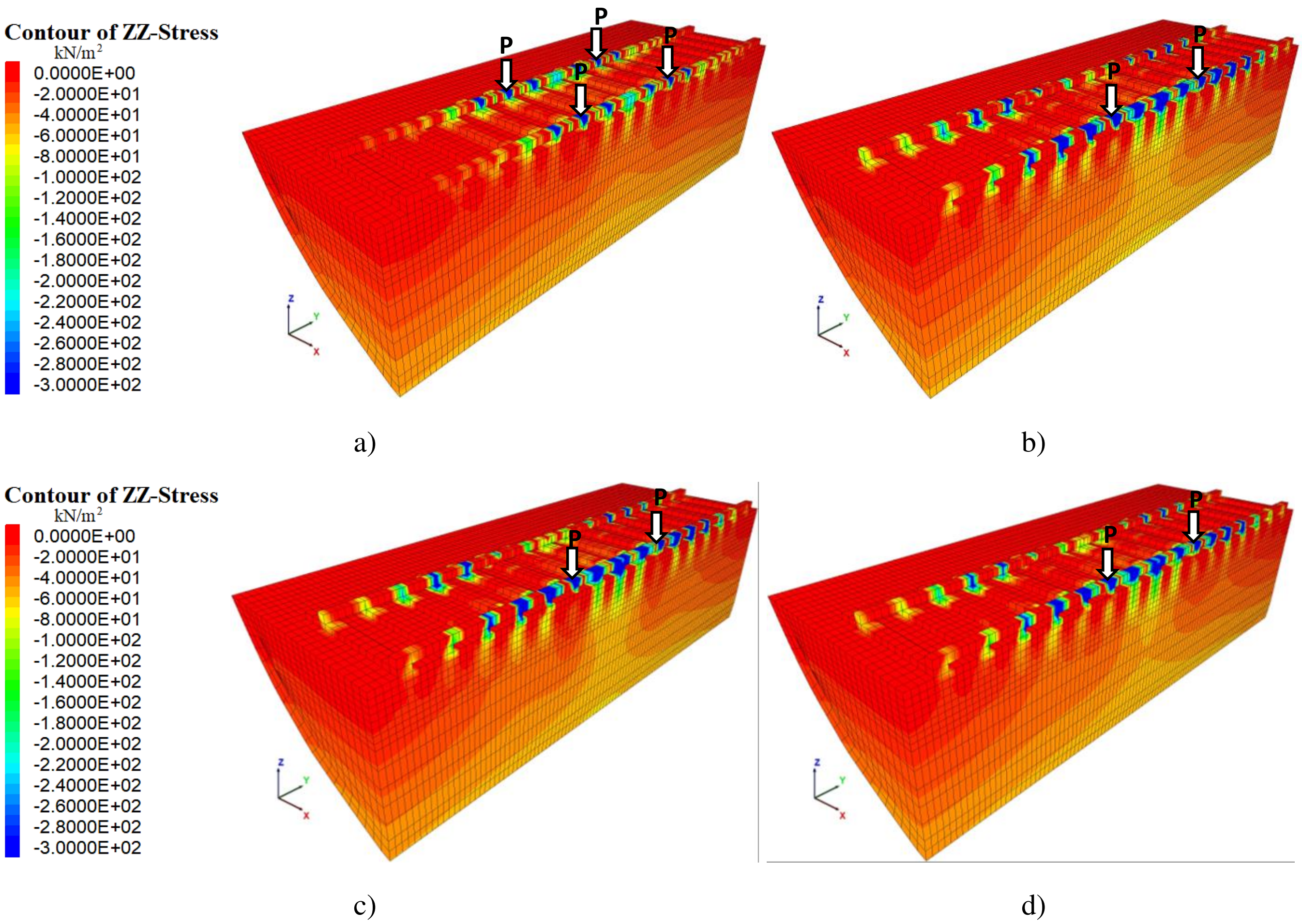

Figure 5. Vertical stress a) case II, b) case III, c) case IV and d) case V

Table 4. Vertical stress of the cases analysed.

Control point	AREMA (2010) (kPa)	Hay (1982) (kPa)	Case I (kPa)	Case II (kPa)	Case III (kPa)	Case IV (kPa)	Case V (kPa)
A (A')*	226.78	459.68	101.1 (109)	161.2 (152)	342.4 (310)	361.1 (306)	367.9 (310)
A (A')**			32.1 (83.5)	31.9 (123.3)	72.7 (233.0)	40.0 (235.1)	98.2 (203.8)
B (B')*	218.54	442.98	72.5 (69.7)	116.8 (97.1)	226.6 (206)	246.5 (182)	251.1 (195.2)
B (B')**			19.5 (41.9)	33.2 (63.9)	58.1 (142.3)	49.3 (199.6)	106.7 (194.9)
C (C')*	174.00	352.70	60.5 (57.9)	93.2 (80.4)	188.4 (166)	204.8 (152)	201.1 (156)
C (C')**			12.8 (40.5)	20.4 (56.8)	32.8 (137.3)	25.8 (184.1)	50.3 (175.5)
D (D')*	91.89	186.25	40.2 (43.2)	67.4 (55.9)	115.8 (105)	129.9 (104)	138.3 (104)
D (D')**			15.7 (31.4)	20.2 (40.5)	31.5 (70.9)	23.1 (78.0)	40.6 (71.7)

*: First cycle; **: After 1000 cycles.

Table 5. Minimum Safety Factors of the cases analysed.

Case	Minimum Safety Factor in subballast or fluid concrete
I	1.45
II	1.43
III	1.28
IV	1.33
V	3.00

Figure 6 (a) shows the vertical displacement at control point A, CP-A (Figure 1), for all the cases analysed. It can be seen, case III shows the largest displacement (6 mm) for the 1000 load cycles simulated, which is in accordance with the FS obtained, since it presented the lowest value of the cases analysed. Figure 6 (b) presents the vertical stress along the track with depth from the base of the sleepers. The data shows 3 prominent incremental peaks, which indicate the point of application of the cyclic load and one at the centre of the model generated by the intersection of the surrounding pressure bulbs.

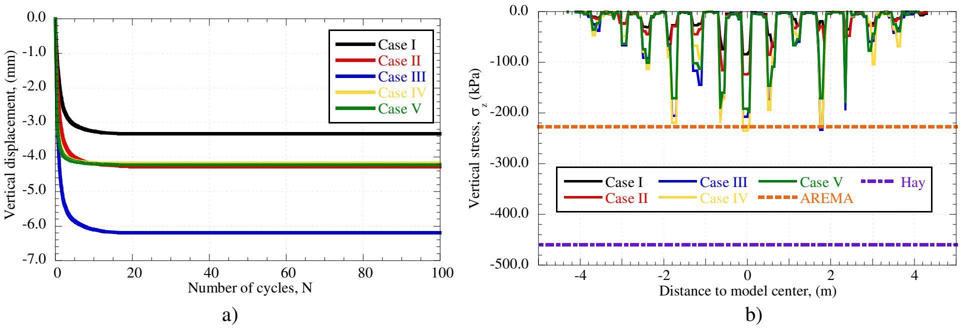

Figure 6. a) Vertical displacement time histories and b) vertical stress measured control point A

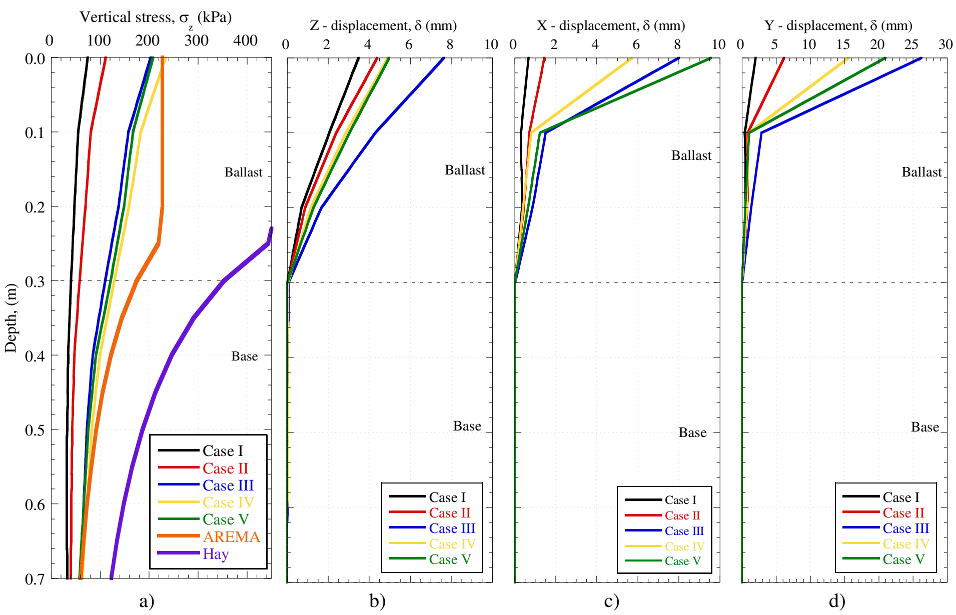

Figure 7. a) Vertical stress with depth and comparison with cases studies, b) Z displacement, c) X displacement and d) Y displacement measured under the sleeper from ballast top

Figure 7 (a) shows the maximum vertical stress with depth from the base of the sleepers for all cases, the dissipation of stress with depth is observed, this is due to the characteristics of the base layer and the compaction of the materials. The stresses calculated agree with the those obtain by AREMA (2010). However, the FS of the most of cases (i.e., I, II, III, ands IV) is less than 1.5. Therefore, it is not possible to fully evaluate the performance of a support system following this criterion. In the other hand the criterion of Hay overestimates the vertical stress, which can lead to very expensive and less efficient construction. The displacements are showed in Figure 7 (b), (c) and (d), indicating a significant decrease in the lower part of the ballast layer, due to the greater confinement with respect to the upper part of this layer.

4 CONCLUSIONS

Due to the cyclic nature of the loading during the operation of urban trains throughout their service life, stress levels close to failure lead to the potential for plastic deformations, as the stresses exceed the linear range in the base-type material or ballast materials. Likewise, these deformations are the cause of the high wear experienced by these materials, mainly in the curved areas, where the stress concentration is higher. Therefore, a design that does not consider the increase in loads due to the geometric layout of the track, as well as the determination of maximum displacements, both elastic and plastic must be considered incomplete. From the cases studied with the numerical model, it was found that replacing the ballast (Case IV) does not significantly attenuate the level of stresses reaching the base-type material, so it was decided to evaluate the replacement of the ballast with a fluid concrete fill (Case V). For the latter, a stabilization trend of the vertical displacement was observed, so that, for this type of track support system, it is necessary to replace both materials (base-type material and ballast) to ensure good track performance, and to minimize maintenance costs. The results of the numerical models satisfactorily capture the stresses when compared to those calculated by AREMA (2010). However, the FS for most of the cases (i.e., I, II, III, and IV) is less than 1.5, which lead to significant plastic deformations (Figure 7), in which the maximum plastic deformation reached in the last unloading stage was 26 mm. Therefore, it is not possible to fully evaluate the performance of a support system following this criterion. In the other hand the criterion proposed by Hay overestimates the vertical stress, which can lead to very expensive and inefficient construction. Although the methodology used in this work is capable of simulating the performance of track support materials, there are some limitations. One aspect that can be improved in this simulation is to include an advanced constitutive model that consider breakage and wear of ballast particles, using a coupled analysis with continuous elements and discrete elements. These data will be compared eventually with those obtained from direct measurements and published in a posteriori and extended publication of this investigation. Finally, it is worth highlighting the importance of further studying the behavior of materials commonly used as track support, in order to design railways in an optimal way, avoiding frequent maintenance.

5 REFERENCES

AREMA 2010. American Railway Engineering and Maintenance-of-Way Association, Volume 1

Burt, G.L. 2007. *Handbook of Geotechnical Investigation and Design Tables,* Taylor & Francis Group, London, UK

CEMEX 2020. Manual del constructor Concretos CEMEX.

Das, A., Bajpai, P. K. 2018. A hypo-plastic approach for evaluating railway ballast degradation. *Acta Geotechnica*, 13(5), 1085-1102.

Hay, W. 1982. *Railroad Engineering. Second Edition*, John Wiley and Sons, Inc., New York.

Indraratna, B., Nimbalkar, S.S. 2013. Stress-Strain Degradation Response of Railway Ballast Stabilized with Geosynthetics. *Journal of Geotechnical and Geoenvironmental Engineering*. 2013.139:684-700.

Itasca Consulting Group 2012. FLAC3D Fast Lagrangian Analysis of Continua, Ver. 5.0 User's Manual, Minneapolis, USA

Liu, H., Zou, D. 2013. Associated generalized plasticity framework for modeling gravelly soils considering particle breakage. *Journal of Engineering Mechanics*, 139(5)

Lysmer J., Kuhlemeyer R. L. 1969. Finite Dynamic Model for Infinite Media, *J. Eng. Mech.*, 95(EM4), 859-877.

Montiel-Varela, G., Domínguez-Vázquez A.C., Gallardo-Hernández, E.A., Bregant, L., García-Illescas, R. 2017. Experimental and numerical study for detection of rail defect. Engineering Failure Analysis. Vol 81 (2017)

Ramos, A., Correia, A. G., Calçada, R., Costa, P. A., Esen, A., Woodward, P. K., Connolly, D.P., Laghrouche, O. 2021. Influence of track foundation on the performance of ballast and concrete slab tracks under cyclic loading: Physical modelling and numerical model calibration. *Construction and Building Materials*, 277, 122245

Sayeed, M.A., Shahin, M.A. 2016. Three-dimensional numerical modelling of ballasted railway track foundations for high-speed trains with special reference to critical speed. *Transportation Geotechnics*. Vol. 6 (2016) 55–65

Sayeed, M., Shahin, M. A. 2022. Dynamic response analysis of ballasted railway track–ground system under train moving loads using 3D finite element numerical modelling. *Transportation Infrastructure Geotechnology*, 1-21.

Selig, E., Waters, J. 1994. *Track geotechnology and substructure management*. Thomas Telford.

Talbot, A.N. 1920. Second Progress Report of the Special Committee to Report on Stresses in Railroad Track, *AREA Proceedings*, Volume 21, 1920, pp.645-814.